

# Mathematical Modelling and Numerical Simulation of Fluid-Magnetic Particle Flow in a Small Vessel

Benchawan Wiwatanapataphee, Kittisak Chayantrakom, and Yong-Hong Wu

**Abstract**—Fluid-solid flow phenomena is an interdisciplinary research area with great technological, commercial and medical importance. One particular application is related to the drug delivery system in which magnetic targeting offers the ability to target a specific site, such as a tumor. This paper presents a mathematical model and a finite element method, based on the Arbitrary Lagrangian Eulerian approach, for studying blood-magnetic particle flow in small vessels. Four models with one, three, five, and nine particles are used to analyze the flow pattern and pressure distribution along the flow direction. Effects of magnetic force on the blood-particle flow are investigated.

**Keywords**—Arbitrary Lagrangian Eulerian, finite element method, fluid-particle flow, magnetic fluids.

## I. INTRODUCTION

CANCER is one of the most insidious and potentially fatal diseases in human being. Many evidences indicate that progressive tumor growth is dependent on angiogenesis which is the process in which new blood vessels develop from an existing vasculature through endothelial cell sprouting, proliferation and fusion [1]. New blood vessels provide nutrients to proliferating cancer cells, which is in favor of tumor growth. Tumor cells need an adequate blood supply in order to perform vital cellular functions. The degree of disturbance of blood flow is thus a good predictor of the course of the disease, and hence regional blood flow measure can permit earlier cancer detection. The modern-day approach to cancer treatment is a multidisciplinary one involving varying combination of surgery, radiation therapy, chemotherapy, and targeted therapies (a new weapon). In

targeted therapies, a medication or drug is controlled to target a specific pathway in the growth and development of a tumor. Although most of the drugs used to date have proven to be successful on small animals such as mice [19, 20], their efficiency in humans remains highly variable from one patient to another. Understanding the flow of blood and drug in the capillary bed is very important for investigating the efficiency of drug treatment as they pass from parent blood vessel to tumor surface via an associated capillary bed. Over the last 15 years, a number of mathematical models for blood vessel formation [3, 4], blood flow and/or particle flow in capillary networks [5, 6, 7, 8, 9, 15, 16, 17] in the area of tumor-induced angiogenesis have been developed. One of these, magnetically targeted drug delivery, involves binding a drug to small biocompatible magnetic particles with diameters less than 5  $\mu\text{m}$ .

Driscoll *et al.* [22] had studied magnetically targeted drug delivery by tracking each individual particle under the influence of Stokes drag force and magnetic force. Grief and Richardson [17] conducted a theoretical analysis of targeted drug delivery using magnetic particles and proposed a two-dimensional network model. In their model, the motion of fluid is described by Poiseuille flow, whereas the motion of a magnetic particle, due to balancing hydrodynamic and magnetic force, is governed by an advection-diffusion equation for the particle concentration. They found that drug targeting can be achieved by pulling magnetic particles to the edge of the vessel, and that the use of magnetically targeted drug delivery with an externally applied magnetic field is appropriate only for targets close to the surface of the body.

However, most existing models do not take into account of the real 3D effect and the interaction between blood flow and magnetic particles, Non-Newtonian behavior of blood and the effect of magnetic forces. Therefore in order to fully understand and control the local flow behavior of blood and particles through the area of tumor-induced angiogenesis, it is essential to develop a sophisticated model and computational technique for the flow analysis. Hence, based on the current development in the field, the objective of this paper is to propose a sophisticated model and computational technique for analyzing the complex flow (blood-particle flow) behavior in tumor-induced capillary networks using the current state-of-the-art computational fluid dynamic (CFD) technology.

Manuscript received March 30, 2007. Revised Manuscript received July 14, 2007. The first author gratefully acknowledges the support of the Thailand Research Fund (TRF) and the support of the Australian government under the 2007 Endeavor Australian Research fellowship. The research is done in collaboration with Mahidol University, Bangkok, Thailand and Curtin University of Technology, Perth, WA, Australia.

B. Wiwatanapataphee is with the Department of Mathematics, Mahidol University, Bangkok, 10400 Thailand (e-mail: scbww@mahidol.ac.th).

K. Chayantrakom is with the Department of Mathematics and Statistics, Curtin University of Technology, Perth, WA 6845 Australia (e-mail: kittisak.chayantrakom@postgrad.curtin.edu.au).

Y.H. Wu is with the Department of Mathematics and Statistics, Curtin University of Technology, Perth, WA 6845 Australia (e-mail: yhwu@maths.curtin.edu.au).

Our model couple the interaction of blood flow with the particle flow using the Arbitrary Lagrangian Eulerian (ALE) formulation. The governing equations for blood flow are the continuity equation and the Navier-Stokes equations. For particle movement, Newton's law is applied. The complete model includes the governing equations for the blood flow, the governing equations for the motion of fine particles, the interaction conditions between blood and particle at the interfaces, and boundary conditions. More specifically, the paper aims to (a) present a mathematical model and an efficient finite element method based on the Arbitrary Lagrangian Eulerian approach for studying blood-magnetic particle flow in a small vessel; (b) analyze the effect of number of particles on the flow pattern and pressure distribution along the flow direction; (c) investigate the effect of magnetic force on the flow pattern of blood and particles and pressure distribution.

## II. GOVERNING EQUATIONS

To study the motion of solid particles immersed in a fluid, we assume that the fluid-solid particle system occupies a bounded domain  $\bar{\Omega}$  in  $\mathbb{R}^3$ . At a typical instant of time  $t$ ,  $Q$  particles occupy  $Q$  closed connected subsets  $\sum_{q=1}^Q \Omega_q \subset \mathbb{R}^3$  which is surrounded by a viscous homogeneous fluid filling the domain  $\bar{\Omega} - \sum_{q=1}^Q \Omega_q$  called the flow-channel area.

In this study we use two coordinate systems: a reference system,  $\Omega$ , where the model is drawn and the particle movement is solved, and a moving mesh system,  $\Omega_{def}$ , corresponding to the deformed mesh of the flow channel, where we simulate the fluid flow. The time evolution of the domain  $\Omega_{def}$  is determined by means of an Arbitrary Lagrangian-Eulerian (ALE) mapping  $\mathbf{x} : \Omega \times \mathbb{R}^+ \mapsto \Omega_{def}$  which maps any point  $(\mathbf{X}, t)$  to its image  $\mathbf{x}(\mathbf{X}, t)$ .

### A. Transformation

In the flow-channel area, the two coordinate systems,  $(X, Y, Z) \in \Omega$  and  $(x, y, z) \in \Omega_{def}$  are connected through a transformation  $T$ . At the initial state at  $t = 0$ , the two mesh systems are assumed to coincide. The transformation  $T$  maps the point initially located at  $(X, Y, Z)$  to the point  $(x, y, z)$  at time  $t$ :

$$\begin{aligned} x &= x(X, Y, Z, t) \\ T : \quad y &= y(X, Y, Z, t) \\ z &= z(X, Y, Z, t). \end{aligned}$$

Suppose that the functions  $x, y,$  and  $z$  are continuous differentiable with respect to  $X, Y, Z$ . Then the infinitesimals  $dX, dY, dZ$  transform into  $dx, dy, dz$

according to

$$\begin{aligned} dx &= x_{,X} dX + x_{,Y} dY + x_{,Z} dZ, \\ dy &= y_{,X} dX + y_{,Y} dY + y_{,Z} dZ, \\ dz &= z_{,X} dX + z_{,Y} dY + z_{,Z} dZ, \end{aligned} \tag{1}$$

where  $(\cdot)_{,X}$  denotes differentiation with respect to  $X$ .

System (1) can be written in matrix form as

$$\begin{bmatrix} dx \\ dy \\ dz \end{bmatrix} = \begin{bmatrix} x_{,X} & x_{,Y} & x_{,Z} \\ y_{,X} & y_{,Y} & y_{,Z} \\ z_{,X} & z_{,Y} & z_{,Z} \end{bmatrix} \begin{bmatrix} dX \\ dY \\ dZ \end{bmatrix}. \tag{2}$$

The  $3 \times 3$  matrix of partial derivatives in (2) is called the Jacobian matrix of the transformation. Denote the matrix by  $\mathbf{J}$ , then

$$\begin{aligned} |\mathbf{J}| &= x_{,X}(y_{,Y}z_{,Z} - y_{,Z}z_{,Y}) - x_{,Y}(y_{,X}z_{,Z} - y_{,Z}z_{,X}) \\ &\quad + x_{,Z}(y_{,X}z_{,Y} - y_{,Y}z_{,X}). \end{aligned}$$

For  $|\mathbf{J}| \neq 0$ , the transformation is invertible and there exists an inverse transformation at time  $t$ , i.e.,

$$\begin{aligned} X &= X(x, y, z) \\ T^{-1} : \quad Y &= Y(x, y, z) \\ Z &= Z(x, y, z). \end{aligned}$$

As in (2), we have

$$\begin{bmatrix} dX \\ dY \\ dZ \end{bmatrix} = \begin{bmatrix} X_{,x} & X_{,y} & X_{,z} \\ Y_{,x} & Y_{,y} & Y_{,z} \\ Z_{,x} & Z_{,y} & Z_{,z} \end{bmatrix} \begin{bmatrix} dx \\ dy \\ dz \end{bmatrix}. \tag{3}$$

From (2), we also have

$$\begin{bmatrix} dX \\ dY \\ dZ \end{bmatrix} = \mathbf{J}^{-1} \begin{bmatrix} dx \\ dy \\ dz \end{bmatrix}, \tag{4}$$

where

$$\begin{aligned} \mathbf{J}^{-1} &= \begin{bmatrix} I_{Xx} & I_{Xy} & I_{Xz} \\ I_{Yx} & I_{Yy} & I_{Yz} \\ I_{Zx} & I_{Zy} & I_{Zz} \end{bmatrix} = \frac{1}{|\mathbf{J}|} \mathbf{K}, \\ \mathbf{K} &= \begin{bmatrix} y_{,Y}z_{,Z} - y_{,Z}z_{,Y} & x_{,Z}z_{,Y} - x_{,Y}z_{,Z} & x_{,Y}y_{,Z} - x_{,Z}y_{,Y} \\ y_{,Z}z_{,X} - y_{,X}z_{,Z} & x_{,X}z_{,Z} - x_{,Z}z_{,X} & y_{,X}x_{,Z} - y_{,Z}x_{,X} \\ y_{,X}z_{,Y} - y_{,Y}z_{,X} & x_{,Y}z_{,X} - x_{,X}z_{,Y} & x_{,X}y_{,Y} - x_{,Y}y_{,X} \end{bmatrix}, \end{aligned} \tag{5}$$

in which the  $I$  syntax is used to emphasize the computation of the Jacobian of the inverse transformation from the inverse of the original Jacobian.

Equating terms in (3) and (4), we obtain

$$\begin{aligned}
 X_{,x} &= (y_{,y}z_{,z} - y_{,z}z_{,y}) / |\mathbf{J}|, \\
 X_{,y} &= (x_{,z}z_{,y} - x_{,y}z_{,z}) / |\mathbf{J}|, \\
 X_{,z} &= (x_{,y}y_{,z} - x_{,z}y_{,y}) / |\mathbf{J}|, \\
 \\ 
 Y_{,x} &= (y_{,z}z_{,x} - y_{,x}z_{,z}) / |\mathbf{J}|, \\
 Y_{,y} &= (x_{,x}z_{,z} - x_{,z}z_{,x}) / |\mathbf{J}|, \\
 Y_{,z} &= (y_{,x}x_{,z} - y_{,z}x_{,x}) / |\mathbf{J}|, \\
 \\ 
 Z_{,x} &= (y_{,x}z_{,y} - y_{,y}z_{,x}) / |\mathbf{J}|, \\
 Z_{,y} &= (x_{,y}z_{,x} - x_{,x}z_{,y}) / |\mathbf{J}|, \\
 Z_{,z} &= (x_{,x}y_{,y} - x_{,y}y_{,x}) / |\mathbf{J}|.
 \end{aligned} \tag{6}$$

These relations are crucial in transforming the calculation results from  $\Omega_{def}$  to  $\Omega$ .

*B. Motion of Fluid-Solid Flow in the Deformed Mesh System*

To study the motion of magnetic particles in the fluid flow channel, we assume that the gravitational force can be neglected and the particle movement is governed by Newton's second law:

$$\begin{aligned}
 m_q \frac{\partial \mathbf{V}_q}{\partial t} &= \mathbf{F}_v + \mathbf{F}_q + \mathbf{F}_{mag}, q = 1, 2, 3, \dots, Q \\
 \mathbf{V}_q \Big|_{t=0} &= \mathbf{0}.
 \end{aligned} \tag{7}$$

The position  $\mathbf{X}_q$  of the center of the  $q$  th particle can be determined by the equation:

$$\begin{aligned}
 \frac{d\mathbf{X}_q}{dt} &= \mathbf{V}_q, q = 1, 2, 3, \dots, Q \\
 \mathbf{X}_q \Big|_{t=0} &= \mathbf{X}_q^0.
 \end{aligned} \tag{8}$$

In equation (7)<sub>1</sub>,  $\mathbf{V}_q$  and  $m_q$  denote the velocity vector and the mass of the  $q$  th particle. The three applied loads, drag force  $\mathbf{F}_v$ , collision force  $\mathbf{F}_q$ , and magnetic force  $\mathbf{F}_{mag}$ , are defined based on the following assumptions:

- All boundaries of particles experience drag force  $\mathbf{F}_v$  from fluid,
 
$$\mathbf{F}_v = -\mathbf{n}_f \cdot (-p\mathbf{I} + \eta(\nabla\mathbf{v} + (\nabla\mathbf{v})^T)) \tag{9}$$
 which consists of the pressure and the viscous drag of the fluid.
- To prevent the collisions among the particles, and the particles and the vessel walls, the particle-particle interaction force  $\mathbf{F}_{q,p}$  and the particle-wall interaction force  $\mathbf{F}_{q,w}$  are applied when the distance between two particles, or between a particle and a wall, is within the order of the element size [21]

$$\mathbf{F}_q = \sum_{p=1, p \neq q}^Q \mathbf{F}_{q,p} + \sum_{w=1}^2 \mathbf{F}_{q,w}, \tag{10}$$

in which

$$\mathbf{F}_{q,p} = \begin{cases} 0, & \text{for } d_{q,p} > R_q + R_p + \alpha \\ \frac{1}{\varepsilon_q} (\mathbf{X}_q - \mathbf{X}_p)(R_q + R_p + \alpha - d_{q,p})^2, & \\ 0, & \text{for } d_{q,p} \leq R_q + R_p + \alpha \end{cases} \tag{11}$$

and

$$\mathbf{F}_{q,w} = \begin{cases} 0, & \text{for } d_{q,w} > 2R_q + \alpha \\ \frac{1}{\varepsilon_w} (\mathbf{X}_q - \mathbf{X}_w)(2R_q + \alpha - d_{q,w})^2, & \\ d_{q,w} \leq 2R_q + \alpha \end{cases} \tag{12}$$

where  $d_{q,p}$  denotes the distance between the centers of the  $q$  th and  $p$  th particles,  $d_{q,w}$  denotes the distance between the centers of the  $q$  th particle and the imaginary particle on the other side of the wall,  $\mathbf{X}_q$  and  $R_q$  are center and radius of the  $q$  th particle,  $\alpha$  is the force range, and  $\varepsilon_q$  and  $\varepsilon_w$  are small positive stiffness parameters.

- To trap magnetic particles (drugs) at the target site, an external magnetic field is applied to generate a magnetic force acting on the particle [25]. This force, which is composed of three components, is governed by the equations:

$$\mathbf{F}_{mag} = \frac{1}{\mu_r} (\mathbf{M} \cdot \nabla) \mathbf{B}, \tag{13}$$

where  $\mu_r$  is the relative permeability of a magnetic material,  $\mathbf{M} = (M_x, M_y, M_z)$  is the magnetic moment of the particle, and  $\mathbf{B} = (B_x, B_y, B_z)$  is the magnetic flux density.

To determine the drag force  $\mathbf{F}_v$  in (9), blood is assumed to be an isotropic, homogeneous incompressible fluid. The motion of the blood is described by the continuity equation and the Navier-Stokes equations

$$\nabla \cdot \mathbf{v} = 0, \tag{14}$$

$$\rho_f \frac{\partial \mathbf{v}}{\partial t} + \rho_f (\mathbf{v} \cdot \nabla) \mathbf{v} - \nabla \cdot \boldsymbol{\sigma} = \mathbf{F}, \tag{15}$$

for  $\mathbf{x}$  in  $\Omega_{def}(t)$  where  $\rho_f$  denotes the blood density,  $\mathbf{v} = [u, v, w]^T$  represents the 3D velocity vector, and  $\mathbf{F}$  is the volume force acting on the fluid. For this model, we neglect the effect of gravitational force and thus  $\mathbf{F} = \mathbf{0}$ . The

quantity  $\sigma$  in equation (15) is the stress tensor given by

$$\sigma = -p\mathbf{I} + \eta(\nabla\mathbf{v} + (\nabla\mathbf{v})^T) \quad (16)$$

where  $\eta$  is the blood viscosity and  $p$  is the blood pressure.

On the wall, the no-slip condition is applied. On the inflow boundary  $\Gamma_{in}$ , the velocity is assumed to be constant, whereas on the outflow boundary  $\Gamma_{out}$ , the stress-free condition is used:

$$\begin{aligned} \mathbf{v} &= \mathbf{v}_0 \text{ on } \Gamma_{in} \\ \sigma \cdot \mathbf{n} &= \mathbf{0} \text{ on } \Gamma_{out}. \end{aligned} \quad (17)$$

For static condition in stationary bodies, the magnetic flux density  $\mathbf{B}$  is governed by Maxwell's equations:

$$\begin{aligned} \nabla \cdot \mathbf{B} &= 0 \\ \nabla \times \mathbf{H} &= \mathbf{0} \end{aligned} \quad (18)$$

where the magnetic flux density  $\mathbf{B}$  and the magnetic field strength  $\mathbf{H}$  are related through the constitutive relation

$$\mathbf{B} = \mu_0\mu_r\mathbf{H} + \mathbf{B}_r, \quad (19)$$

in which  $\mathbf{B}_r = \mu_0\mu_r\mathbf{M}$  denotes a residual flux density,  $\mu_0$  is the permeability in vacuum.

From the first equation of (18), the magnetic flux density can be determined from a vector potential by  $\mathbf{B} = \nabla \times \mathbf{A}$  which identically satisfies the first equation of (18). Using the identity

$$\nabla \times (\nabla \times \mathbf{A}) = \nabla(\nabla \cdot \mathbf{A}) - \Delta\mathbf{A},$$

and the Coulomb gauge  $\nabla \cdot \mathbf{A} = 0$ , the second equation of (18) takes the form

$$\nabla \times (\mu_0^{-1}\mu_r^{-1}\nabla \times \mathbf{A} - \mathbf{M}) = \mathbf{0}, \forall \mathbf{x} \in \Omega_{def}$$

or

$$\Delta\mathbf{A} = -\nabla \times (\mu_0\mu_r\mathbf{M}), \quad (20)$$

which is the vector-valued Poisson equation for the magnetic potential  $\mathbf{A}$ .

Due to the movement of the coordinate system, the mesh velocity  $\Psi = (\Psi_x, \Psi_y, \Psi_z)$  is introduced in the deformed domain  $\Omega_{def}$ . To guarantee a smoothly varying distribution of the nodes, we assume that the nodes on  $\partial\Omega_q$  move with the particle (no slip) and that each component of the mesh velocity in the fluid channel is governed by a Laplace equation:

$$\nabla^2\Psi = 0, \forall \mathbf{x} \in \Omega_{def}. \quad (21)$$

The above equation is to smooth gradient of the mesh velocity over the domain so as to reduce mesh distortion. Once the mesh velocity components are determined, we can determine the smoothed deformed mesh for the flow channel at each time instant by updating the coordinates of the nodes according to the following formulae

$$\begin{aligned} x &= X + \int_0^t \Psi_x dt, \\ y &= Y + \int_0^t \Psi_y dt, \\ z &= Z + \int_0^t \Psi_z dt. \end{aligned} \quad (22)$$

Another condition that needs to be specified is that the fluid, particle and mesh move with the same velocity on the particle boundaries, i.e.,

$$\Psi = \mathbf{v} = \mathbf{V}_q \text{ on } \partial\Omega_q. \quad (23)$$

We now have the strong coupled problem for the fluid-particle flow in the drug delivery system. These equations are solved to yield  $\mathbf{V}_q$  in  $\Omega$  and  $\mathbf{v}, p, \mathbf{A}, \Psi$  in  $\Omega_{def}$ .

### C. Finite Element Formulations

The weak formulation of the fluid flow problem is to find  $(\mathbf{v}, p, \mathbf{A}, \Psi) \in \mathfrak{S} \equiv [H^1(\Omega_{def})]^3 \times H^1(\Omega_{def}) \times [H^1(\Omega_{def})]^3 \times [H^1(\Omega_{def})]^3$  in the deformed mesh system at each time instant such that all the Dirichlet boundary conditions are satisfied and  $\forall (\hat{\mathbf{v}}, \hat{p}, \hat{\mathbf{A}}, \hat{\Psi}) \in \mathfrak{S}^0 \equiv \{(\hat{\mathbf{v}}, p, \hat{\mathbf{A}}, \hat{\Psi}) \in \mathfrak{S} \mid \hat{\mathbf{v}} = \mathbf{0} \text{ on } \partial\Omega_{def_v}, \hat{p} = 0 \text{ on } \partial\Omega_{def_p}, \hat{\mathbf{A}} = \mathbf{0} \text{ on } \partial\Omega_{def_A}, \text{ and } \hat{\Psi} = \mathbf{0} \text{ on } \partial\Omega_{def_\Psi}\}$ ,

$$\int_{\Omega_{def}} \hat{p}(\nabla \cdot \mathbf{v}) d\Omega = 0, \quad (24)$$

$$\begin{aligned} \int_{\Omega_{def}} (\rho_f \hat{\mathbf{v}} \cdot \frac{\partial \mathbf{v}}{\partial t} + \eta \nabla \hat{\mathbf{v}} : \nabla \mathbf{v} + \rho_f \hat{\mathbf{v}} \cdot (\mathbf{v} \cdot \nabla) \mathbf{v} - p \nabla \cdot \hat{\mathbf{v}}) d\Omega &= \int_{\partial\Omega_{def}} \hat{\mathbf{v}} \cdot (\sigma \cdot \mathbf{n}) ds, \end{aligned} \quad (25)$$

$$\int_{\Omega_{def}} (\nabla \hat{\mathbf{A}} : \nabla \mathbf{A} - \hat{\mathbf{A}} \cdot \nabla \times (\mu_0\mu_r\mathbf{M})) d\Omega = 0, \quad (26)$$

and

$$\int_{\Omega_{def}} (\nabla \hat{\Psi} : \nabla \Psi) d\Omega = 0, \quad (27)$$

where  $\partial\Omega_{def_v}, \partial\Omega_{def_p}, \partial\Omega_{def_A}$ , and  $\partial\Omega_{def_\Psi}$  are the parts of boundary where the velocity, the pressure, the magnetic potential, and the mesh velocity are specified. It should also be addressed that various surface integral terms, arising in the formulation, vanish as the test functions involved in the terms are zero on the boundary.

Since the computations are conducted in the reference coordinates,  $\Omega$ , we need to transform equations (24)-(27) in the deformed coordinates to those equations in the reference coordinates. Through this and using (17)<sub>2</sub>, we obtain

$$\int_{\Omega} \hat{p}(\nabla \cdot \mathbf{v}) |\mathbf{J}| d\Omega = 0, \quad (28)$$

$$\int_{\Omega} (\rho_f \hat{\mathbf{v}} \cdot \frac{\partial \mathbf{v}}{\partial t} + \eta \nabla \hat{\mathbf{v}} : \nabla \mathbf{v} + \rho_f \hat{\mathbf{v}} \cdot (\mathbf{v} \cdot \nabla) \mathbf{v} - p \nabla \cdot \hat{\mathbf{v}}) |\mathbf{J}| d\Omega = \int_{\partial\Omega} \hat{\mathbf{v}} \cdot (\sigma \cdot \mathbf{n}) |\mathbf{J}| ds,$$

$$-p\nabla \cdot \hat{\mathbf{v}} \Big| \mathbf{J} \Big| d\Omega = 0, \quad (29)$$

$$\int_{\Omega} (\nabla \hat{\mathbf{A}} : \nabla \mathbf{A} - \hat{\mathbf{A}} \cdot \nabla \times (\mu_0 \mu_r \mathbf{M})) \Big| \mathbf{J} \Big| d\Omega = 0, \quad (30)$$

and

$$\int_{\Omega} (\nabla \hat{\Psi} : \nabla \Psi) \Big| \mathbf{J} \Big| d\Omega = 0, \quad (31)$$

where the derivatives of the unknown functions  $\Psi_i (i = x, y, z)$  are determined by the following expressions:

$$\begin{aligned} \Psi_{i,x} &= \Psi_{i,x} I_{X,x} + \Psi_{i,y} I_{Y,x} + \Psi_{i,z} I_{Z,x}, \\ \Psi_{i,y} &= \Psi_{i,x} I_{X,y} + \Psi_{i,y} I_{Y,y} + \Psi_{i,z} I_{Z,y}, \\ \Psi_{i,z} &= \Psi_{i,x} I_{X,z} + \Psi_{i,y} I_{Y,z} + \Psi_{i,z} I_{Z,z}, \end{aligned} \quad (32)$$

and for the test functions:

$$\begin{aligned} \hat{\Psi}_{i,x} &= \hat{\Psi}_{i,x} I_{X,x} + \hat{\Psi}_{i,y} I_{Y,x} + \hat{\Psi}_{i,z} I_{Z,x}, \\ \hat{\Psi}_{i,y} &= \hat{\Psi}_{i,x} I_{X,y} + \hat{\Psi}_{i,y} I_{Y,y} + \hat{\Psi}_{i,z} I_{Z,y}, \\ \hat{\Psi}_{i,z} &= \hat{\Psi}_{i,x} I_{X,z} + \hat{\Psi}_{i,y} I_{Y,z} + \hat{\Psi}_{i,z} I_{Z,z}. \end{aligned} \quad (33)$$

The derivatives of other unknown functions  $u, v, w, A_x, A_y,$  and  $A_z$  are defined in the same way as those of the  $\Psi_i$  functions.

### III. NUMERICAL RESULTS AND DISCUSSION

In a two dimension case, the magnetic potential is assumed to have a nonzero component only in the direction perpendicular to the plane, i.e.,  $\mathbf{A} = (0, 0, A_z)$ . On  $\partial\Omega_q$  and  $\partial\Omega$ , the magnetic potential is set to zero, that is,  $A_z = 0$ .

The magnetization  $\mathbf{M} = (M_x, M_y)$  for the magnetic source is given by  $M_x = 0, M_y = 5 \times 10^4 \text{ A}\cdot\text{m}^{-1}$ , and for the magnetic particles

$$\begin{aligned} M_x &= a \arctan \left( \frac{b}{\mu_0 \mu_r} A_{z,y} \right), \\ M_y &= a \arctan \left( -\frac{b}{\mu_0 \mu_r} A_{z,x} \right), \end{aligned} \quad (34)$$

where  $a$  and  $b$  are two material parameters.

From (13), the magnetic force,  $\mathbf{F}_{mag} = (F_{mag_x}, F_{mag_y})$ , is given by

$$\begin{aligned} F_{mag_x} &= \frac{1}{\mu_r} (M_x A_{z,yx} + M_y A_{z,yy}), \\ F_{mag_y} &= \frac{1}{\mu_r} (-M_x A_{z,xx} - M_y A_{z,xy}). \end{aligned} \quad (35)$$

To understand the blood-particle flow in a small vessel, a 2D domain with one, three, five, and nine particles are used. The computation domain is a horizontal channel with height

of  $6.2 \mu\text{m}$  and length of  $45 \mu\text{m}$ . The particles are circular with diameter of  $0.5 \mu\text{m}$ . Blood is assumed to flow into the channel with speed  $1.85 \text{ cm/s}$  from the left to the right. The fluid properties are typical of human blood with the viscosity  $\eta$  of  $0.0035 \text{ Pa}\cdot\text{s}$  and the density  $\rho_f$  of  $1060 \text{ kg}\cdot\text{m}^{-3}$ . All particles are assumed to be solid with the density of  $1112 \text{ kg}\cdot\text{m}^{-3}$ . The relative permeability  $\mu_r$  is  $5 \times 10^3$  for the magnet particles and  $0.99998$  for the tissue in the blood vessel. The material parameters  $a$  and  $b$  are  $1 \times 10^{-4}$  and  $3 \times 10^{-5}$ , respectively.

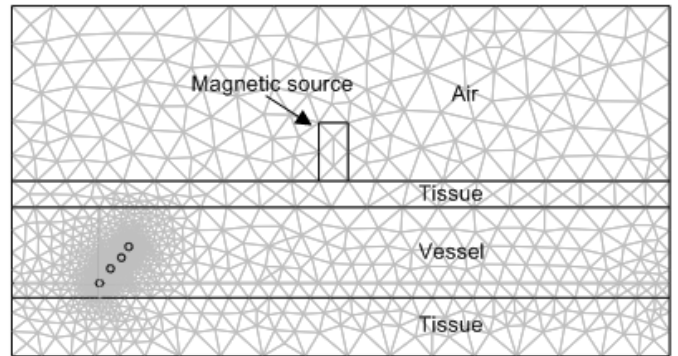


Fig. 1 The 2D geometry of the blood vessel with a magnetic source at the middle of the vessel and its finite element mesh

The Arbitrary Lagrangian Eulerian approach is used to handle the dynamics of deforming geometry and the moving boundaries. New mesh coordinates on the channel area are calculated based on the movement of the particles. The Navier-Stokes equations are formulated in the moving coordinate system. Particle interactions and particle collisions are neglected. Via the simulations of the model we can describe the flow pattern and pressure distribution in the particle-fluid system.

Fig. 1 shows the finite element mesh and the external magnetic field applied to the system. The computation domain consists of 3519 elements with 1791 nodes.

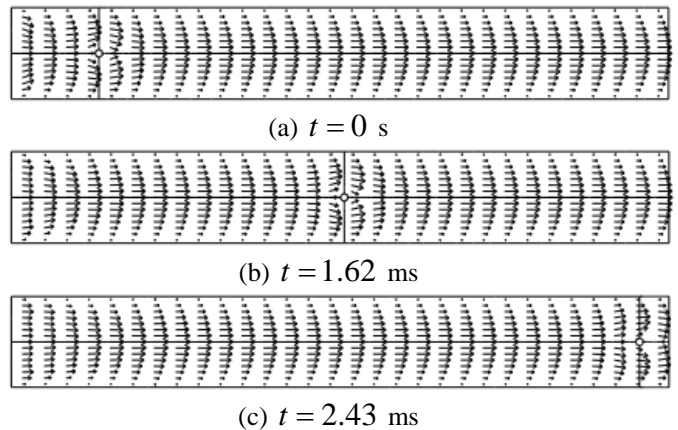


Fig. 2 Velocity profiles at various instants of time for the case with one particle

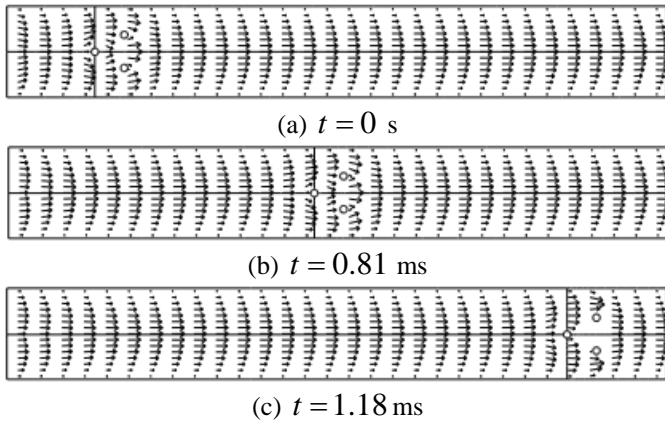


Fig. 3 Velocity profiles at various instants of time for the case with three particles

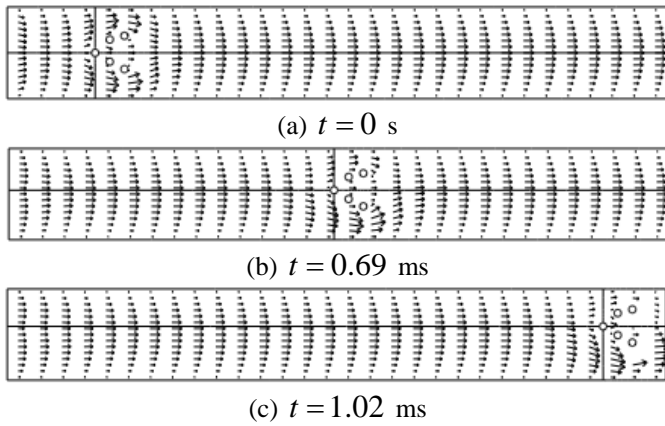


Fig. 4 Velocity profiles at various instants of time for the case with five particles

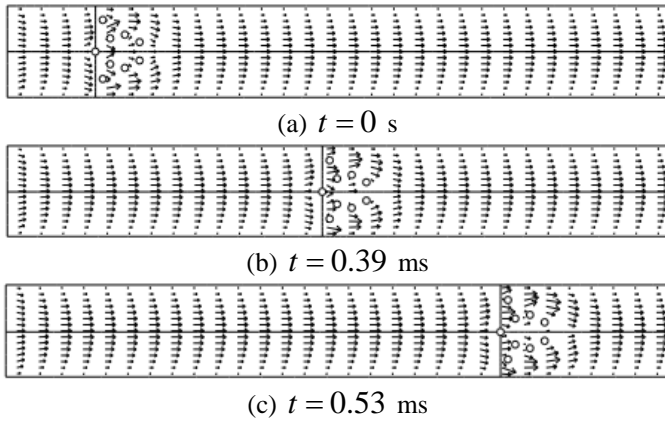


Fig. 5 Velocity profiles at various instants of time for the case with nine particles

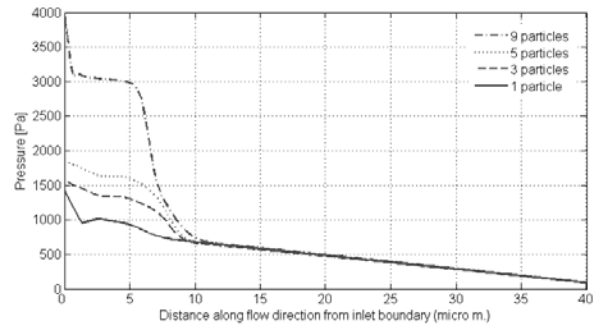


Fig. 6 Pressure profiles along the flow direction at  $t = 0$  s

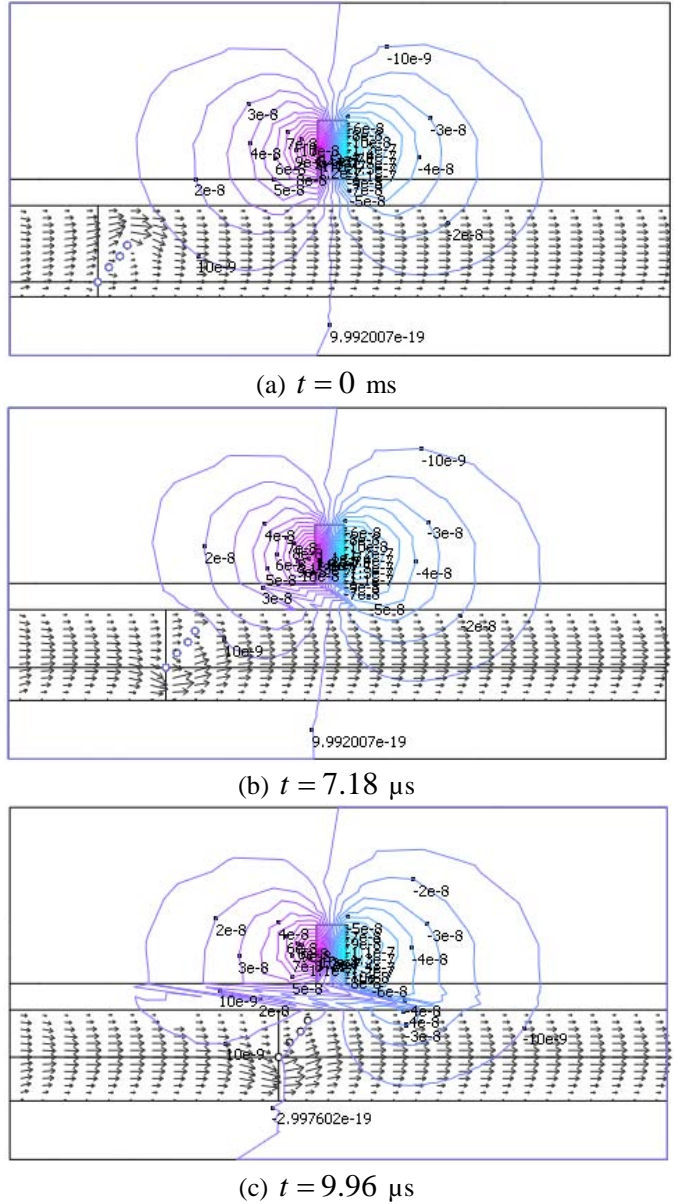


Fig. 7 Velocity profiles at various instants of time for the case with four magnetic particles

Fig. 2-5 show the velocity distributions for the models with one, three, five, and nine particles, respectively, at the absence of the external magnetic field. In these cases, the particles

flow in the axial direction. Fig. 6 shows the pressure distribution along the axis of the tube at  $t = 0$  for various cases with different number of particles in the fluids. It is noted that with the increase of particle number, the pressure required on the entry of the tube increases significantly. Fig. 7 shows the velocity profile of fluid and the particle motion for the case with four particles at the presence of an external magnetic field. It is clearly noted that the model can simulate the flow of particles toward the targeted region.

## REFERENCES

- [1] W. Risau, "Mechanisms of angiogenesis," *Nature*, no. 386, pp. 671--74, 1997.
- [2] D. Balding, and D. L. S. McElwain, "A mathematical model of tumour-induced capillary growth," *J. Theor. Biol.*, vol. 114, pp. 53--73, 1985.
- [3] H. M. Byrne, and M. A. J. Chaplain, "Mathematical models for tumour angiogenesis: numerical simulations and nonlinear wave solutions," *Bull. Math. Biol.*, vol. 57, pp. 461--86, 1995.
- [4] H. A. Levine, S. Pamuk, B. D. Sleeman, and M. Nielsen-Hamilton, "Mathematical modeling of capillary formation and development in tumour angiogenesis: penetration into the stroma," *Bull. Math. Biol.*, vol. 63, pp. 801-63, 2001.
- [5] S. R. McDougall, A. R. A. Anderson, M. A. J. Chaplain, and J. A. Sherratt, "Mathematical modeling of flow through vascular networks: implications for tumour-induced angiogenesis and chemotherapy strategies," *Bull. Math. Biol.*, vol. 64, pp. 673-702, 2002.
- [6] T. Alarcon, H. Byrne, and P. Maini, "A cellular automaton model for tumour growth in inhomogeneous environment," *J. Theor. Biol.*, vol. 225, pp. 257-74, 2003.
- [7] A. Stephanou, S. R. McDougall, A. R. A. Anderson, and M. A. J. Chaplain, "Mathematical modeling of flow in 2D and 3D vascular networks: applications to anti-angiogenic and chemotherapeutic drug strategies," *Math. Comput. Model.*, vol. 41, pp. 1137-56, 2005.
- [8] S. R. McDougall, A. R. A. Anderson, and M. A. J. Chaplain, "Mathematical modeling of dynamic adaptive tumour-induced angiogenesis: clinical implications and therapeutic targeting strategies," *J. Theor. Biol.*, to be published.
- [9] A. Stephanou, S. R. McDougall, A. R. A. Anderson, and M. A. J. Chaplain, "Mathematical modeling of the influence of blood rheological properties upon adaptive tumour-induced angiogenesis," *Math. Comput. Model.*, to be published.
- [10] S.G. Etemad, A. S. Mujumdar, and B. Huang, "Viscous dissipation effects in entrance region heat transfer for a power law fluid flowing between parallel plates," *Int. J. Heat and Fluid Flow*, vol. 15, no. 2, pp. 122-132, 1994.
- [11] G. J. F. Smit, and J. P. Du Plessis, "Pressure drop prediction of power law fluid through granular media," *Journal of Non-Newtonian Fluid Mechanics*, vol. 72, pp. 319-323, 1997.
- [12] G. J. F. Smit, and J. P. Du Plessis, "Modelling of Non-Newtonian purely viscous flow through high porosity synthetic foams," *Chemical Engineering Science*, vol. 54, pp. 645-654, 1999.
- [13] G. J. F. Smit, and J. P. Du Plessis, "Modelling of Non-Newtonian flow through isotropic porous media," *Mathematical Engineering in Industry*, vol. 8, pp. 19-40, 2000.
- [14] S. Petkova, A. Hossain, J. Naser, and E. Palombo, "CFD modelling of blood flow in portal vein hypertension with and without thrombosis," in *Third International Conference on CFD in the Minerals and Process Industries CSIRO*, Melbourne, Australia, 10-12 Dec. 2003.
- [15] E. K. Ruuge, and A. N. Rusetski, "Magnetic fluids as drug carriers: targeted transport of drugs by a magnetic field," *Journal of Magnetism and Magnetic Materials*, vol. 122, pp. 335-339, 1993.
- [16] Q. A. Pankhurst, J. Connolly, S. K. Jones, and J. Dobson, "Applications of magnetic nanoparticles in biomedicine," *J. Physics D*, vol. 36, pp. R167-R181, 2003.
- [17] A. D. Grief, and G. Richardson, "Mathematical modelling of magnetically targeted drug delivery," *Journal of Magnetism and Magnetic Materials*, vol. 293, no. 1, pp. 455-463, 2005.
- [18] J. Dobson, "Magnetic Nanoparticles for drug delivery," *Drug Development Research*, vol. 67, pp. 55-60, 2006.
- [19] S. Goodwin, C. Peterson, C. Hoh, and C. Bittner, "Targeting and retention of magnetic targeted carriers (MTCs) enhancing intra-arterial chemotherapy," *J. of Magnetism and Magnetic Materials*, vol. 194, pp. 132-139, 1999.
- [20] K. J. Widder, R. M. Morris, G. Poore, D. P. Howard Jr., and A. E. Senyei, "Tumor remission in Yoshida sarcoma-bearing rats by selective targeting of magnetic albumin microspheres containing doxorubicin," *Pro. Natl. Acad. Sci. USA*, vol. 78, no. 1, pp. 579--581, 1981.
- [21] P. Singh, D. D. Joseph, T. I. Hesla, R. Glowinski, and T. W. Pan, "A distributed Lagrange multiplier/fictitious domain method for viscoelastic particulate flows," *J. Non-Newtonian Fluid Mechanics*, vol. 91, pp. 165-188, 2000.
- [22] C. F. Driscoll, R. M. Morris, A. E. Senyei, K. J. Widder, and G. S. Heller, "Magnetic targeting of microspheres in blood flow," *Microvasc. Res.*, vol. 27, pp. 353-369, 1984.
- [23] E. M. Knobbe, "Mesh movement governed by entropy production," in *Proceedings, 13th International Meshing Roundtable*, Williamsburg, VA, Sandia National Laboratories, pp.265-276, September 19-22, 2004.
- [24] C. M. Oldenburg, S. E. Borglin, and G. J. Moridis, "Numerical simulation of ferrofluid flow for subsurface environmental engineering applications," *Transport in Porous Media*, vol. 38, pp. 319-344, 2000.
- [25] A. H. Felix, and M. Sylvain, "Suggested shape for a first generation endovascular untethered microdevice prototype," in *Proceedings of the 2005 IEEE Engineering in Medicine and Biology 27th Annual Conference*, Shanghai, China, September 1-4, 2005, pp. 1286-1288.
- [26] R. E. Rosensweig, *Ferrohydrodynamics*, Dover Publications, New York, 1997.